

# A Neuronal Gamma Oscillatory Signature During Morphological Unification in the Left Occipitotemporal Junction

Jonathan Levy,<sup>1,2,3,4,\*</sup> Peter Hagoort,<sup>2,5</sup> and Jean-François Démonet<sup>3,4,6</sup>

<sup>1</sup>The Gonda Multidisciplinary Brain Research Center, Bar Ilan University, Ramat Gan, Israel

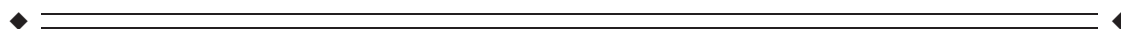
<sup>2</sup>Donders Institute for Brain, Cognition and Behaviour, Radboud University Nijmegen, Nijmegen, The Netherlands

<sup>3</sup>Inserm UMR825, Imagerie cérébrale et handicaps neurologiques, Toulouse, France

<sup>4</sup>Université de Toulouse, UPS, Toulouse, France

<sup>5</sup>Max Planck Institute for Psycholinguistics, Nijmegen, The Netherlands

<sup>6</sup>Department of Clinical Neurosciences, Leenaards Memory Center, CHUV and University of Lausanne, Lausanne, Switzerland



**Abstract:** Morphology is the aspect of language concerned with the internal structure of words. In the past decades, a large body of masked priming (behavioral and neuroimaging) data has suggested that the visual word recognition system automatically decomposes any morphologically complex word into a stem and its constituent morphemes. Yet the reliance of morphology on other reading processes (e.g., orthography and semantics), as well as its underlying neuronal mechanisms are yet to be determined. In the current magnetoencephalography study, we addressed morphology from the perspective of the unification framework, that is, by applying the Hold/Release paradigm, morphological unification was simulated via the assembly of internal morphemic units into a whole word. Trials representing real words were divided into words with a transparent (true) or a nontransparent (pseudo) morphological relationship. Morphological unification of truly suffixed words was faster and more accurate and additionally enhanced induced oscillations in the narrow gamma band (60–85 Hz, 260–440 ms) in the left posterior occipitotemporal junction. This neural signature could not be explained by a mere automatic lexical processing (i.e., stem perception), but more likely it related to a semantic access step during the morphological unification process. By demonstrating the validity of unification at the morphological level, this study contributes to the vast empirical evidence on unification across other language processes. Furthermore, we point out that morphological unification relies on the retrieval of lexical semantic associations via induced gamma band oscillations in a cerebral hub region for visual word form processing. *Hum Brain Mapp* 35:5847–5860, 2014. © 2014 Wiley Periodicals, Inc.

**Key words:** morphology; visual word form area; reading; oscillations; unification; magnetoencephalography



## INTRODUCTION

In the past decades, much theoretical and empirical efforts have been focused on the representational nature of morphologically complex words (i.e., words that can be decomposed into separate components; e.g., “player” = “play” + “er”) in various language systems. However, researchers have long been in disagreement regarding the nature of such words’ organization in the

---

\*Correspondence to: Jonathan Levy, The Gonda Multidisciplinary Brain Research Center, Bar Ilan University, Ramat Gan, Israel. Email: yoniilevy@gmail.com

Received for publication 21 October 2013; Revised 4 July 2014; Accepted 9 July 2014.

DOI: 10.1002/hbm.22589

Published online 15 July 2014 in Wiley Online Library (wileyonlinelibrary.com).

mental storage, that is, as separate morphemic constituents [e.g., Taft and Forster, 1975], or as full forms [Butterworth, 1983]. Furthermore, even among those who support the morphemic view, the parameters that determine and influence the putative morphological process (e.g., its reliance on orthography [i.e., letters] or on semantics [i.e., lexical semantic associations]) were far from indisputable. The theory of morphological processing suggests that along the course of language acquisition, the visual system recognizes at multiple occurrences certain words, which share orthography and meaning (e.g., “play,” “player,” “playful,” “replay”), and maps them in terms of their morphemic constituents [Rastle et al., 2000]. This cerebral mapping of form and meaning gradually translates into the outstanding expertise of the visual system to automatically decompose complex words into morphemic units. Some claim that true morphological decomposition relies on both form and meaning, and thereby, theoretically, should only operate on morphologically transparent words (that is not to be confounded with orthographic transparency which represents grapheme-to-phoneme regularity), that is, words that share a similar meaning with their constituents (e.g., a “player” is someone who plays). Accordingly, decomposition would not be expected to occur in pseudomorphological constructions in which the relationship between the full form and the stem is semantically non-transparent (NT) (e.g., a “corner” is not someone who corns). Hence, for true morphological processing to take place, the brain would access both orthography (the morphemic constituents) and semantics (the semantic relationship between the constituents). Yet others claim that the visual system not only decomposes truly morphological words but also pseudomorphological words, thereby proclaiming an orthographic coreliance. In more detail, present theories of morphological processing can be summarized by four main approaches [Beyersmann et al., 2012]: (1) the obligatory decomposition account [Taft, 2003], according to which morphologically structured words are automatically decomposed into their morphemic subunits regardless of their internal semantic relationship; (2) the supralexic account [Giraudo and Grainger, 2001], claiming that the morphemic decomposition occurs after the semantic access; (3) the form-then-meaning account [Crepaldi et al., 2010], which claims inversely, that first morphemic decomposition occurs, and then semantic access; and (4) the hybrid model [Diependaele et al., 2009; Feldman et al., 2009], stating that morpho-orthographic and morphosemantic decomposition can occur in parallel at early initial processing stages in visual word recognition.

To date, research has primarily applied priming paradigms in which primes and targets do or do not share a semantic relationship. Nevertheless, there have been conflicting findings showing that pseudomorphological pairs (i.e., with a NT relationship) and real morphological pairs (i.e., with a transparent relationship) produce similar priming effects [Rastle et al., 2004], or alternatively—do not

[Diependaele et al., 2009; Feldman et al., 2009; Morris et al., 2007]. Findings of similar priming effects provide support to the orthography-based view, whereas different priming effects support the semantic-based view. Although ample evidence from time-resolving neuroimaging methods (electroencephalography, magnetoencephalography) during the past decade has reshaped theories of morphological processing [e.g., Lavric et al., 2007, 2012; Lehtonen et al., 2011; Morris et al., 2007, 2008; Martin and Thierry, 2008; Solomyak and Marantz, 2009], it has not resolved the debate but has instead complicated and detailed its outlook. Namely, the various event-related potentials/fields findings have not always corroborated and have even sometimes contradicted each other particularly as for the contribution of semantics. Several studies reported the recruitment of semantics during earlier components (e.g., N250) [Lavric et al., 2012; Morris et al., 2007; Martin and Thierry, 2008] while other studies refuted this finding [Lavric et al., 2007; Lehtonen et al., 2011; Morris et al., 2008] (in Morris et al., 2008, note however, the differential semantic contribution during the two phases of N250). Even during later components (e.g., N400), some reported a semantic effect [Morris et al., 2007] while others not [Lavric et al., 2007]. Altogether, we reason that addressing morphology from a different perspective, at both the framework and the mechanism levels, may contribute to the overall understanding of this process.

To start with, the assumption of decomposition possibly implies a following step of assembly of the word segments into a coherent word. This fits well into the MUC (Memory, Unification, Control) framework [Hagoort, 2005], which assumes the retrieval of representational units (e.g., morphemes) from memory and their combination into a larger unit (e.g., a word). This process relies on a mechanism of information binding at multiple levels of processing such as syntactic, semantic, and phonological. At various points of this dynamic clipping process, alternative binding candidates are often evoked by automatic associations (e.g., lexical-semantic or syntactic associations), meaning that an inhibitory mechanism selects one candidate from the different unification options. This perspective is in line with linguistic theories and models, which highlight the role of combinatorial operations that assemble the basic components into larger structures [Bresnan, 2001; Chomsky, 1995; Jackendoff, 2002; Joshi and Schabes, 1997; MacDonald et al., 1994]. In this study, we simulate morphological processing using an approach which is reversed to the traditional decompositional paradigms (i.e., morpheme decomposition). Specifically, we contend that assembling morphemic constituents into a single word could straightforwardly probe the role of semantics for morphology, instead of relying on indirect priming techniques. Notwithstanding the contribution of the decompositional approach, the unification framework is particularly explicit from a computational perspective, and is as well compatible with a large series of empirical findings in the sentence processing literature, in the

neuropsychological literature on aphasia [Vosse and Kempen, 2000], and even with the famous “neural binding problem” in visual neuroscience [for an overview, see Engel and Singer, 2001]. Although unification operations have particularly focused on syntax, they apply also to other processing levels in language comprehension (e.g., semantics and phonology). Here, we tested the unification framework on morphological processing and, therefore, term it morphological unification. While true morphological unification would require the successful semantic addition of a stem and a morpheme, a pseudomorphological unification would trigger no such semantic addition as the morpheme then bears no semantic valence that could complement the stem. Hence, if the brain “blindly” adds up morphemic units to form a real word, then, we would observe identical processing of morphologically transparent and NT words. However, if semantics plays a pivotal role during the process of morphological unification, we would then observe differential processing between morphologically transparent and NT words.

Furthermore, to date, the methodological approaches to studying morphological processing have evolved from theory, through behavioral paradigms, through blood oxygenation level dependent (BOLD) neuroimaging of putative neuronal generators, and temporally evoked activity related to such mechanisms. Here, however, we focused our analysis on the measure of induced neuronal oscillations which reliably reflect cortical processing [Buzsaki and Draguhn, 2004], and are partly or totally cancelled out in time domain averaging (e.g., evoked potentials or fields), but not in spectral power averaging. Specifically, we probed gamma band activity (40–150 Hz) for two important reasons: First, they best correlate with functional magnetic resonance imaging (fMRI) BOLD responses, can capture important aspects of information processing in the cortex, and convey a relatively reliable anatomical-functional mapping [Crone et al., 1998; Foster and Parvizi, 2012; Voytek et al., 2010]. Second, gamma band oscillations constitute a precise marker of orthographic and semantic processing during single-word recognition [Gaillard et al., 2009; Mainy et al., 2008; Vidal et al., 2012; Vidal et al., 2014]. Third, induced activity appears with a jitter in latency from one trial to the next and is sustained in time, thereby reflecting processes evolving over hundreds of milliseconds. Empirical findings suggest that this activity results from intrinsic network interactions within the brain (rather than from external drive) that engage integrative functions such as perceptual inference, top-down attention, and decision making [for a review, see Donner and Siegel, 2011 and Tallon-Baudry and Bertrand, 1999]. Hence, induced gamma band oscillations may precisely account for the processing studied here, and additionally, reliably locate it to neuronal clusters of interest which have been previously highlighted by both functional neuroimaging and by neuroanatomical studies. Finally, the use of MEG, in addition to its characteristics of good spatial resolution with high temporal sampling (thereby ostensibly combin-

ing the singular main advantages of fMRI and EEG), has become more prevalent for studying morphology, as it is claimed to reflect heightened sensitivity for lexical processing [Pylkkänen and Marantz, 2003]. Using MEG for the purpose of this study should, therefore, enable a precise temporal characterization of the steps involved during morphological unification, and additionally assign these functional steps to certain neuronal populations.

We, therefore, used MEG to record ongoing brain activity while participants performed a morphological unification procedure followed by a prompt lexical-decision task (e.g., is “dark” + “er” a real word?). To ensure that the task would trigger morphological unification rather than simple reading, we used the Hold/Release paradigm which proved to be efficient in engaging working memory resources for probing various cognitive processes [Martin et al., 2010; Thierry et al., 1998, 2003a, 2003b]. We, therefore, presented the suffix first as to increase the involvement of working memory during the “hold” phase. We reasoned that by doing so participants would necessarily engage in morphological unification. If instead, suffix were presented last, this would most probably simulate a process more similar to fluent and automatic reading. Furthermore, under the latter design participants would most likely automatically activate many of the set of words beginning with the stem (and not just uniquely the stem word itself). To prevent such plausible a scenario and to rather trigger morphological unification, it was crucial in the current paradigm to apply the counter-ecological design of presenting the suffix first. Thus, to probe the role of semantic access during morphological unification, truly suffixed words were contrasted with pseudosuffixed words. We hypothesized that a local power increase in gamma-band oscillations would take place for truly- (and not for pseudo-) suffixed words in the left occipitotemporal cortex, a major hub of reading processing [Dehaene and Cohen, 2011; Price and Devlin, 2011].

## MATERIALS AND METHOD

### Participants

Sixteen healthy right-handed and native-Dutch subjects (four males, average age  $20.62 \pm 2.47$  years) with normal or corrected-to-normal vision participated in the experiment. None of the participants had a history of neurological or psychiatric disorders. The study was approved by the local ethics committee, and a written informed consent was obtained from the subjects before the experiment according to the Declaration of Helsinki, and received monetary compensation.

### Stimuli

Stimuli were generated using Presentation software (Neurobehavioral systems, Albany) in a dimly lit room and

subtended a horizontal visual angle of  $\sim 2.5^\circ$ . They were projected on an LCD monitor placed at a viewing distance of 70 cm. Responses were delivered by response pads. The stimuli consisted of a common subset of word for all participants, but randomized differently for each participant. Words were presented only once to prevent automatic stimulus–response learning or repetition-suppression effect. All words were segmented into a stem and a suffix morpheme, and presented sequentially in the reversed order than the standard, that is, the suffix first, followed by the stem. In this way, the subject had to perform morphological unification to try and build up a word from those two segments. The words were divided into genuine morphological words, that is, the word and the stem had a transparent semantic dependence (English example: “player,” Dutch example: “rijping”), and to pseudo morphological words, that is, the word and the stem had a NT semantic dependence (English example: “corner,” Dutch example: “paling”). Moreover, whereas transparent (labeled T) words (e.g., the Dutch word “rijping” meaning “maturation” in English) have always consisted of meaningful stems (e.g., “rijp” meaning “mature” in English), NT (labeled NT) words (e.g., the Dutch words “paling” and “kever” meaning “eel” and “beetle” in English, respectively) were equally subdivided into items consisting of a meaningful stem (e.g., the Dutch stem “pal” actually functions as a word in itself, meaning “paw!” in English, thereby labeled as pseudotransparent, or “PT”) and into items with no meaningful stem (e.g., “kev” has no literal meaning in Dutch). The latter consisted of words which are made of letter sequences that may have a suffix function in other words but in reality the words cannot be split apart from a morphological point of view (hence labeled as pseudosuffixed, or “PS”), and morphology of the considered language recognizes them as monocomponent lexical entities. In this case, unification could be experimentally achieved but would be based solely on an orthographic (or superficial in memory terms) process (and we did not focus on this process in our study). Thus, this study probed morphological unification by addressing the processing differences between T and NT words, while NT words were themselves subdivided in two types (PT and PS) to control for the plausibly evoked bias by stems’ semantic valence.

For the three word categories (T, PT, and PS), 240 Dutch nouns were preselected with a lemma frequency [see Baayen et al., 1993] of 192.19 (mean)  $\pm$  107.13 (median: 163.50), 215.73 (mean)  $\pm$  117.22 (median: 177), and 232.857 (mean)  $\pm$  227.08 (median: 177), respectively, without a statistically significant difference between the three categories (ANOVA:  $P = 0.72$ ). The total letter length of the words (stem + morpheme) was 7.98 (mean)  $\pm$  1.08 (median: 8), 6.56 (mean)  $\pm$  1.01 (median: 7), and 6.25 (mean)  $\pm$  1.08 (median: 7), respectively, with a statistically significant difference between the three observations (ANOVA,  $P = 0.001$  corrected; post hoc  $t$ -tests pointing out the difference between T and PT or PS [ $P < 0.001$  corrected], but not between PT and PS [ $P = 0.43$ ]). Furthermore, for the stimuli pairs containing genuine stems, stem frequencies were

computed: for T words, stem frequency was  $1900 \pm 2911$  and for PT words (note that by definition PS items lack any stem)  $1716 \pm 2580$ ; there was no significant statistical difference between the two observations ( $P = 0.77$ ).

## Experimental Procedure

Each trial began with a fixation cross presented for 600–933.33 ms (first presentation after pause presented for 2600–2933.33 ms), followed by the presentation of a morpheme (for 100 ms), a blank SOA (600 ms) and a stem (100 ms). The jitter controlled for plausible anticipation of stimulus onset timing. All stimuli were presented randomly. The subjects were engaged in a lexical decision task; hence, 240 supplementary control stimuli/trials were added. The latter items were not analyzed, and consisted of pairs of stimuli which when unified together, would not represent any real Dutch word. Subjects could respond as soon as the second item appeared, that is, the stem. Responses indicated trials’ termination and lasted for no longer than 2100 ms. Participants observed a crosshair in between trials, during which they were allowed to make eye movements or blinks if needed. They were trained on the task with 30 training trials (different words than during the experiment) before measurement. After blocks of 30 trials, participants were allowed to pause. They initiated the start of each new trial block by a button press. In total, each subject performed 480 trials (240 words and 240 pseudowords as control) in a total measurement time of approximately 40 min. The reports were through right-hand button press on a response pad, and were counter-balanced across subjects between the middle/index fingers of the response hand, in the aim of controlling for differences in the motor representations of each finger.

## MEG Recordings

Ongoing brain activity was recorded (sampling rate, 1200 Hz) using a whole-head CTF MEG system with 275 DC SQUID axial gradiometers (VSM MedTech, Coquitlam, British Columbia, Canada) while subjects were laid in a supine position. Head position was monitored using three coils that were placed at the subject’s left ear, right ear, and nasion. Bipolar EEG channels were used to record horizontal and vertical eye movements as well as the cardiac rhythm for the subsequent artifact rejection. To relate the MEG data to the cerebral locations with high precision, a full-brain anatomical magnetic resonance image (MRI) was acquired for each subject using a three dimensional T1-weighted scan sequence (flip angle,  $15^\circ$ ; voxel size, 1.0 mm in-plane;  $256 \times 256$ ; 164 slices; repetition time: 0.76 s; echo time: 5.3 ms). The anatomical MRIs were recorded using a 1.5 T whole-body scanner (Siemens, Avanto), with anatomical reference markers at the same locations as the head position coils during the MEG recordings for aligning the MEG and the MRI coordinate systems.



### Stratification

To minimize effects of fluctuations in response time (RT) on the spectral analyses, we performed a post hoc stratification of the data based on the RT values. The goal of procedure was to assure that RT variance would not bias the comparison between the two tested conditions (i.e., transparent and NT). The stratification procedure was done at the subject level (on a common pool of words randomized differently for each participant) as we used a two-level statistical approach of within subject statistics (between conditions), and then a random test statistic was performed by pooling the *t*-values over all subjects against the standard normal distribution by applying a permutation procedure. Hence, stratifying the data at the subject level for proceeding with the first test would be the appropriate procedure, as being sensitive to between conditions effects. The outcome of the stratification was a subset of trials with an identical distribution of RT values across the subsets in each of the two conditions. This approach has been adjusted from Roelfsema et al. [Roelfsema et al., 1998] and a similar strategy has been successfully applied before in our previous study [Levy et al., 2013]. For every participant, we binned the observations in each condition, while the bin centers were obtained by dividing the range of all RT values into four equally spaced bins with equal bin centers. In this way, each of the observations fell within one of the bins, for which we selected a subset of observations such that across the two conditions, the number of observations was identical. From the condition with the lowest number of observations in a given bin, all *N* observations constituting that particular bin were selected for the stratified sample. From the other condition, a subset of *N* observations was randomly drawn from the observations constituting that particular bin. Consequently, the distribution of the new pool of trials became equal on the feature of RT. This new pool was used for all analyses described in this article.

### Spectral Analysis

The analysis was performed using MATLAB 7 (MathWorks, Natick, MA) and the FieldTrip toolbox [Oostenveld et al., 2011]. Incorrect trials or trial segments containing eye blinks, saccades, muscle artifacts, and signal jumps were rejected in an automatized partial procedure retaining trial segments superior and equal to 300 ms. The partial procedure allowed us to maximize the “clean” data segments for further analysis. We applied tapers to each time window and calculated time-frequency representations (TFRs) of power for each trial using a Fast Fourier Transform applied to short sliding time windows; data were analyzed in alignment to stimulus onset. Power estimates were, then, averaged across tapers. Because the width of the frequency bands observed in physiological responses typically scales with the center frequency, we analyzed two frequency ranges separately: 2–40 and 40–

150 Hz. For the frequencies 2–40 Hz, we used a Hanning taper and applied a fixed time window of 0.5 s, resulting in a spectral resolution of 2 Hz. For the higher-frequency band (40–150 Hz), we applied five multitapers [Percival and Walden, 1993] using a fixed window length of 0.2 s, resulting in a frequency smoothing of 15 Hz. Induced activity was computed by subtracting the evoked response from every single trial. The power values were calculated for the horizontal and vertical component of the estimated planar gradient and then summed [Bastiaansen and Knösche, 2000]. The horizontal and vertical components of the planar gradients were calculated for each sensor using the signals from the neighboring sensors thus approximating the signal measured by MEG systems with planar gradiometers. The planar field gradient simplifies the interpretation of the sensor-level data because the maximal signal typically is located above the source [Hämäläinen et al., 1993]. The planar gradient power estimates were subsequently averaged over trials for a given condition.

### Source Analysis

For the analysis of the neuronal sources, we used an adaptive spatial filtering method called beamforming [Gross et al., 2001] and relied on partial canonical correlations. Using each participant’s anatomical MRI, a brain volume was created and then divided into a regular grid. The grid positions were obtained by a linear transformation of the grid positions in a canonical 1 cm grid. This canonical grid was based on a template brain (Montreal Neurological Institute), and for each subject, we computed the linear transformation optimally aligning the subject’s brain volume to the template brain, using SPM8 (<http://www.fil.ion.ucl.ac.uk/spm>). We applied the inverse of this linear transformation to the grid positions of the canonical grid to obtain subject-specific dipole grids. This procedure facilitates the group analysis, because no spatial interpolation of the volumes of reconstructed activity is required. For each grid position, we constructed spatial filters. These filters have the property that they optimally pass activity from the location of interest, while other activity, which is present in the data, is suppressed. To compute the lead field matrices, we used a single-shell volume conduction model, based on the shape of the inside of the skull [Nolte, 2003]. The inside of the skull was derived from each individual subject’s structural MRI, which was spatially aligned to the MEG sensors. Despite the fact that in this volume conduction model there is no truly magnetically silent direction, we excluded the most silent direction from the lead fields, as this direction potentially picks up a lot of noise.

To analyze the location of the sources accounting for the significant sensor level effects, we computed the cross-spectral density matrix between all MEG sensor pairs from the Fourier transforms of the tapered data epochs at the two frequency-bands where we had found significant

sensor-level effects: narrow- and broad-band gamma. For each subject, and within each of the two frequency bands, we identified the frequency bin that yielded the most extreme  $t$ -value (for power comparisons), averaged across sensors. Spatial filters were constructed for each grid location, based on the identified frequency bin, and the Fourier transforms of the tapered data epochs were projected through the spatial filters. When analyzing at the coordinate level (virtual channel), we proceeded similarly with beamforming but this time we relied on a linear constrained minimum variance beamformer. Time-frequency analysis was performed with the virtual channel at the coordinates of interest.

### Statistical Analysis

Statistical significance of the power values was assessed similarly at the sensor and at the source levels. It was assessed using a randomization procedure [Maris and Oostenveld, 2007]. This nonparametric permutation approach does take the cross-subject variance into account, because this variance is the basis for the width of the randomization distribution. This approach was chosen as it does not make any assumptions on the underlying distribution, and it is unaffected by partial dependence between neighboring time-frequency pixels. Specifically, the procedure was as follows:  $t$ -values representing the contrast between the conditions were computed per subject, channel, frequency and time. Subsequently, we defined the test statistic by pooling the  $t$ -values over all subjects. Here, we searched time-frequency clusters with effects that were significant at the random effects level after correcting for multiple comparisons along the time and the frequency dimensions. Testing the probability of this pooled  $t$ -value against the standard normal distribution would correspond to a fixed effect statistic. However, to be able to make statistical inference corresponding to a random effect statistic, we tested the significance of this group-level statistic by means of a randomization procedure: We randomly multiplied each individual  $t$ -value by 1 or by  $-1$  and summed it over subjects. Multiplying the individual  $t$ -value with 1 or  $-1$  corresponds to permuting the original conditions in that subject.

This random procedure was reiterated 2000 times to obtain the randomization distribution for the group-level statistic. For each randomization, only the maximal and the minimal cluster-level test statistic across all clusters were retained and placed into two histograms, which we address as maximum (or minimum, respectively) cluster-level test statistic histograms. We then determined, for each cluster from the observed data, the fraction of the maximum (minimum) cluster-level test statistic histogram that was greater (smaller) than the cluster-level test statistic from the observed cluster. The smaller of the two fractions was retained and divided by 2000, giving the multiple comparisons corrected significance thresholds for

a two-sided test. The proportion of values in the randomization distribution exceeding the test statistic defines the Monte Carlo significance probability, which is also called a  $p$ -value [Nichols and Holmes, 2002; Maris and Oostenveld, 2007]. This cluster-based procedure allowed us to obtain a correction for multiple comparisons at all sensor and source analyses. Finally, to apply this statistical approach to the temporal power curves for the selected virtual sensor (Fig. 3B, right panel), the comparison was computed over 10 temporal samples (from 0 to 500 ms) averaged in the NBR.

## RESULTS

### Behavioral Results and RT Stratification

The subjects performed the lexical decision task on the transparent (T) and the NT trials with a mean RT of  $796.67 \pm 95.52$  ms and  $855.08 \pm 99.09$  ms post second item onset ( $P < 10^{-6}$ ), respectively (Fig. 1, left lower panel). Mean accuracy for the two tasks was  $93.12 \pm 4.19\%$  and  $82.20 \pm 8.21\%$ , respectively ( $P < 10^{-6}$ ). To proceed for further spectral analysis while minimizing the effect of variance of the RT and accuracy factors, we analyzed only correct responses, and applied the above described stratification procedure (see Materials and Methods: Stratification) on the RTs, and kept for further analysis only the output data: after this procedure, RTs of selected trials were  $809.03 \pm 95.16$  ms and  $809.9 \pm 96.13$  ms, respectively, without a significant statistical ( $P > 0.2$ ) difference (Fig. 1, right lower panel). After the stratification procedure as well as the rejection of incorrect trials, signal and ocular artifacts, the trials kept for further analysis constituted  $59.38 \pm 7.99\%$  of the original dataset of trials.

### Frequency-Localizer Contrast (T/NT vs. Baseline)

Neuronal network dynamics are characterized by rhythmic oscillatory activity [Buzsaki and Draguhn, 2004]. Using MEG, we measured narrow-band (NGR standing for narrow gamma response) and broad-band gamma response (BGR standing for broad gamma response); the latter has been closely related to underlying population spiking activity [Ray and Maunsell, 2011] and is assimilated as a proxy for active cortical processing [Lachaux et al., 2012]. To constrain the coming analyses to functional rhythmic activity, we first quantified the post-stimulus neural induced oscillatory response as compared to its pre-stimulus baseline response level (intertrial period). We averaged power responses across all sensors and applied the tests for the two combined main conditions as to maximize statistical power and as at such gross level statistics localizer (all sensors averaged, versus baseline). It was not expected that differences between conditions would be expressed at such all-sensors localizer contrast. Therefore,

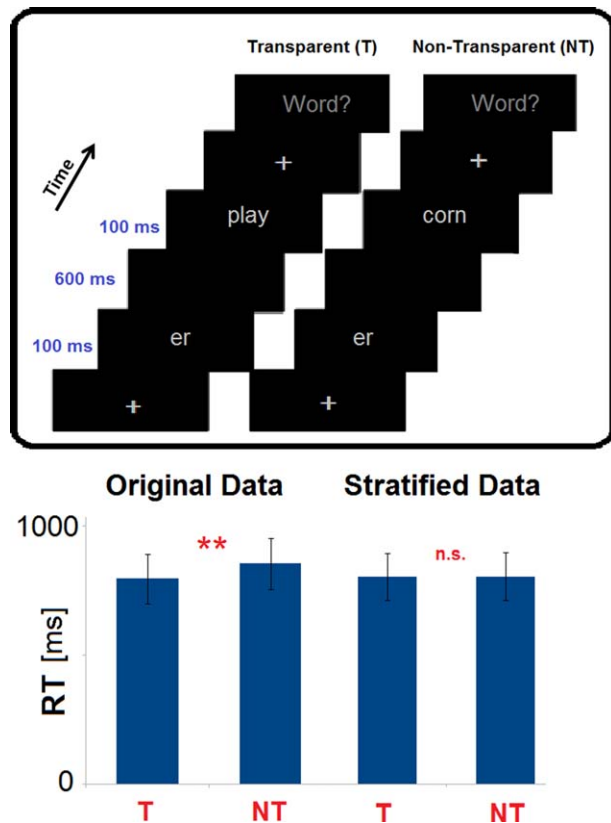


**Figure 1.**

Experimental design and behavioral results. (Upper panel) Design: Experimental paradigm of the morphological unification procedure, prompted by a lexical decision task. (Lower panel) Left: Original mean response times and (Right) stratified mean response times used for further analyses. Error-bars represent  $\pm 1$  SD. [Color figure can be viewed in the online issue, which is available at [wileyonlinelibrary.com](http://wileyonlinelibrary.com).]

for the localizers (conditions contrasted to baseline), we maximized statistical power by considering the two PT and PS subconditions as one NT condition, and by averaging across all sensors (Fig. 2A) as a first step, and across the significant time-frequency windows at the second step (Fig. 2B).

Figure 2A illustrates time-frequency statistical maps of the MEG activity recorded over all sensors during the course of the trial, in the high gamma-band (40–150 Hz) range. The neural response time-frequency statistics map highlights effects for both T and NT conditions (both effects were  $P < 0.01$ , corrected); in this map one could distinguish two oscillatory bands: NGR (60–85 Hz) and BGR (85–150 Hz), so as to explicitly avoid overlapping ranges. Based on those two bands, it was also noticeable that patterns differed across time; the map was, therefore, divided into three time-frequency windows after stem onset: the early BGR (50–200 ms), later NGR (200–500 ms) and latest sustained NGR (500–800 ms).

We then investigated the topographical and source maps (Fig. 2B) in those three TFR windows which illustrated very distinct spatial and cortical effects. Results are suggestive of three functional processes: (1) an early BGR in the bilateral occipital cortex (the bilateral inferior occipital and lingual gyri, BA 18, MNI coordinates  $-22 -90 -12$ ,  $-22 -82 -8$ ,  $26 -78 -16$ ,  $38 -86 -16$ ), plausibly accounting for general visual-feature sensory processing; (2) an early NGR in the left occipitotemporal cortex (hereafter termed LOT; namely, the left cuneus, BA 17, MNI coordinates  $-20 -80 0$ ), plausibly accounting for linguistic (potentially, morphosemantic) processing; and (3) a late NGR in the L-PM (the left precentral gyrus, BA 6, MNI coordinates  $-30 -10 52$ ), plausibly accounting for response-driven motor activity. All topographical and source effects were at a threshold of  $P < 0.01$  correction.

### Morphological Processing (T vs. NT & PT vs. PS)

To probe the neural processing underlying semantic access during morphological processing, we reasoned that such differences would manifest at the cortical level, and in the putatively linguistically functional time window (window 2, in Fig. 2A). By contrast, it was not expected that such differences would manifest in the putatively visual (1) and motor (3) windows. Likewise, it was considered that if oscillatory effects were to diverge between subconditions (PT and PS), those could be revealed at the source level. First, source reconstruction was performed while contrasting power changes in the matched samples conditions T and NT (PT and PS combined). Conforming with our expectation, the statistics at the early BGR and the later sustained NGR windows (1 and 3) yielded insignificant values ( $P > 0.5$  and  $P > 0.8$ , respectively), whereas the first NGR window showed a significant ( $P = 0.01$ , corrected) difference between T and NT, with T showing higher activation localized in the left posterior ventral occipitotemporal cortex (MNI coordinates  $-20 -80 0$ , the left cuneus, BA 17, extending anteriorly toward the left lingual gyrus, BA 18) (Fig. 3A). Second, source reconstruction was also performed in the second pair of matched samples conditions (PT and PS). The rationale behind such additional analysis was that given the meaningful stems comprised in the T and PT conditions (e.g., meaningful Dutch stems “rijp” and “pal,” respectively), these could elicit activity driven by their meaning. By contrast, the PS subcondition consisted of stems without meaning (e.g., “kev” means nothing in Dutch). Hence, to control for differences which may have been driven by meaningful versus meaningless stem processing rather than by morphological unification, differences were also studied between the matched-samples PT and the PS conditions. However, no statistical differences ( $P > 0.35$ ) were found across the cortex at either three windows.

Although our working hypothesis was that effects for morphological unification would best be mirrored through

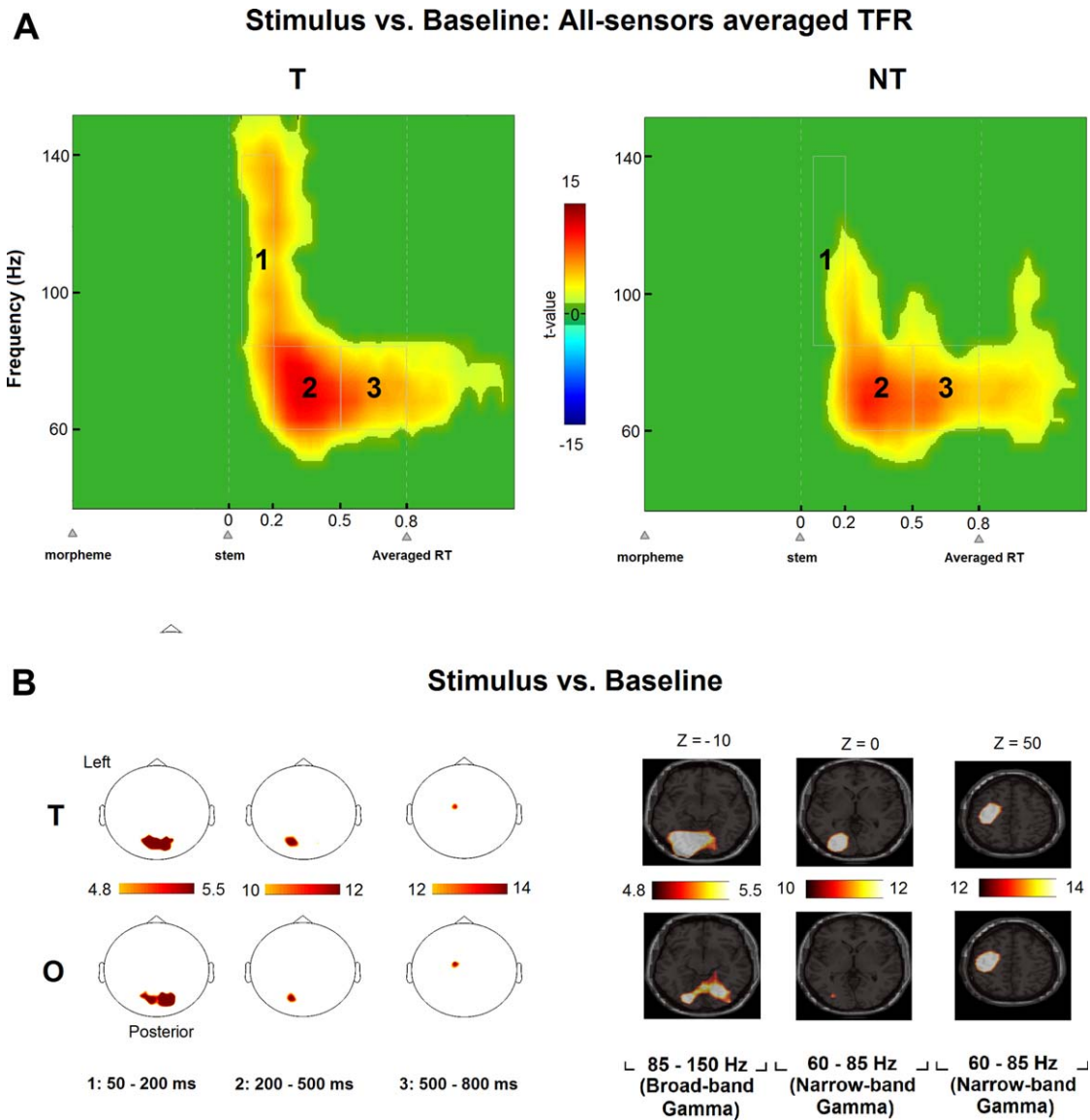


**Figure 2.**

Transparent (T) or Nontransparent (NT) conditions versus baseline activity. **(A)** Frequency-localizer contrast: Time-frequency statistical representation (TFR) maps of 40–150 Hz induced oscillatory activity averaged across all sensors. Color bars illustrate masked significant modulations ( $P < 0.01$ , corrected for multiple comparisons). The maps illustrate induced oscillatory activity modulation from the moment of morpheme presentation (–700 ms) through stem presentation (0 ms) until after response button press (approx. 809 ms); this activity is contrasted with baseline activity ([–1200 –700] ms). The analysis was performed with stimulus-aligned data and was stratified

for reaction time. Morpheme/stem onset time and average response time are indicated on the time axis with a gray triangle and a dashed line. Gray rectangles illustrate on the statistical map three windows: (1) early broad-band gamma, (2) early narrow-band gamma and (3) late narrow-band gamma power modulations. **(B)** Sensor and source activity. (Left panel) Scalp topographies and (Right panel) overlaid cortical axial (MNI template) representations, both illustrate significant clusters ( $P < 0.01$ , corrected) for both T and NT conditions, in the three time-frequency windows of interests (see at the bottom) illustrated in panel (A).

gamma band oscillations, we also considered it supplementary to test whether such unification could be also expressed as power modulation in the lower frequency

ranges. Hence, a localizer contrast (versus baseline) was also performed for the frequency range of 1–40 Hz and detected frequency suppression peaks at the alpha



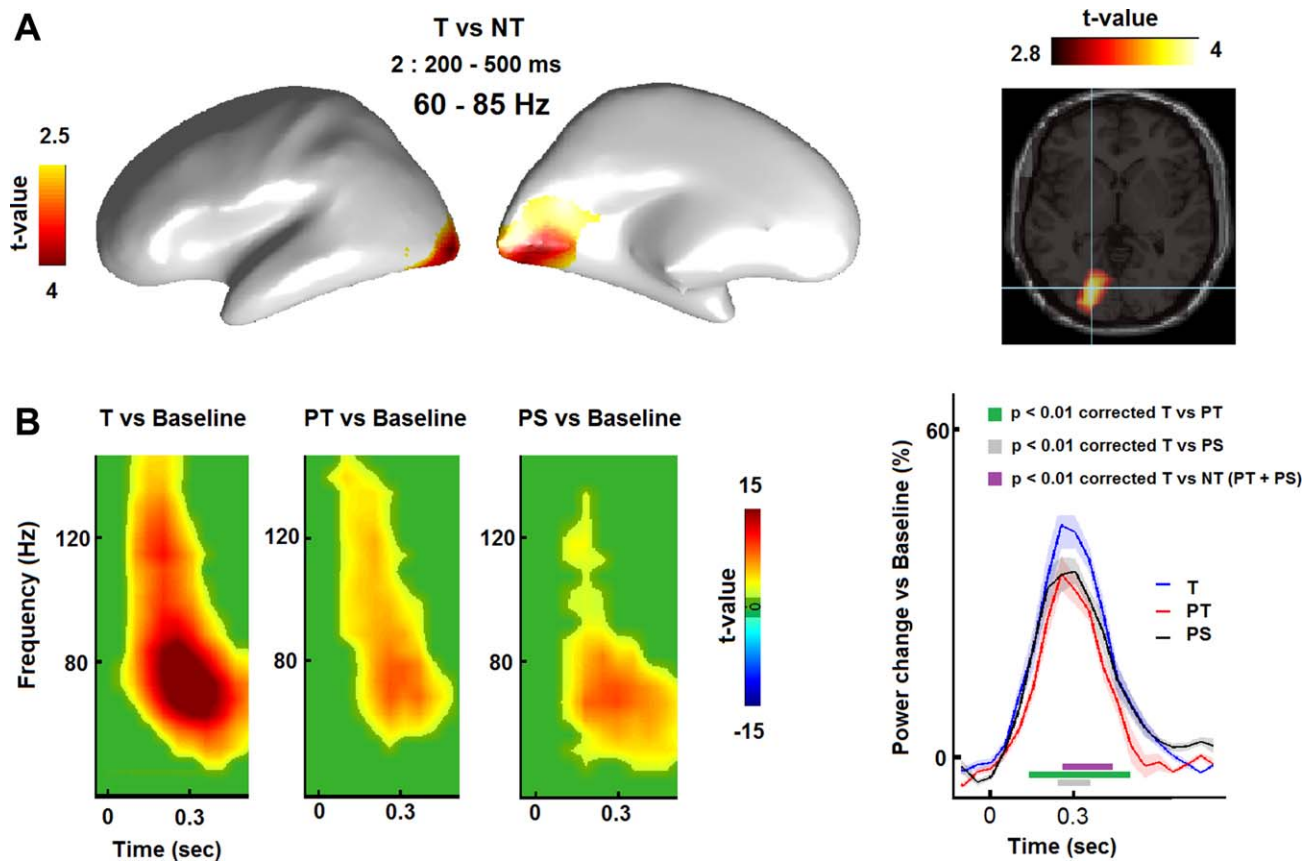


**Figure 3.**

Morphological processing: Transparent (T) versus Nontransparent (NT). **(A)** Source reconstruction of the T versus NT contrast: overlaid cortical surface (left) and axial (right) MNI template representations of the left hemisphere reveal cortical clusters ( $P = 0.01$ , corrected) of the contrast T versus NT in the second selected time-frequency window of interest (i.e., 60–85 Hz; 200–500 ms) as revealed in Figure 2. Color bars illustrate masked significant modulations. **(B)** Virtual channel TFR: On the left side, TFRs of activity filtered from the coordinates of inter-

est illustrate the T, PT, and PS conditions versus baseline (masked  $P < 0.01$ , corrected). On the right side, virtual channel plots represent the temporal evolution of power change of the three conditions averaged in the narrow-gamma band (60–85 Hz). Shades represent standard error of the mean power values, while green or black rectangles indicate statistically significant values ( $P < 0.01$ , corrected) on the time axis rendered by the different contrasts.

(8–10 Hz), lower beta (16–20 Hz), and higher beta (28–32 Hz), all in the approximate time window of 300–600 ms. However, comparing T and NT at the source level in the time-frequency windows of interest yielded the following statistics: in the alpha ( $P > 0.10$ ), in the lower beta ( $P > 0.09$ ), and in the higher beta ( $P > 0.25$ ). Furthermore, testing for plausible stem meaning effect at the lower frequencies, differences between the PT and PS conditions yielded no statistical differences ( $P > 0.45$ ) at either three windows. Hence, the following analyses will focus on induced oscillatory power in the first NGR window (2) as the aforementioned analyses suggest that other time-frequency ranges were not successful in conveying morphological unification.

### Virtual Sensor Analyses in the LOT (T/PT/PS vs. baseline & T vs. PT vs. PS)

The beamformer found that the activity peaked in the posterior LOT (MNI coordinates  $-20 -80 0$ ; Fig. 3A). A virtual sensor was, therefore, computed for these coordinates. Then, TFRs were computed for T, and for the two subconditions of NT, namely PT and PS (Fig. 3B, left panels). Temporal power curves (Fig. 3B, right panel) illustrate power evolution (power change relative to baseline) in the NGR from the stem's temporal onset until 500 ms for T, PT, and PS. Nonparametric statistics revealed significant effects between T and the two other subconditions which were temporally extended for the T versus PT contrast.

The latter overlapped with the T versus PS significant statistics at the time window of 240–360 ms. Nevertheless, to reliably test for statistical differences, matched sampling tests were also performed, namely T versus NT (two sub-conditions combined) as well as PT and PS. The first yielded significant differences in the time window of 260–440 ms ( $P < 0.001$ , corrected), whereas the latter yielded insignificant differences (no clusters in the permutation statistics).

Finally, there was an inherent mismatch in word length (i.e., total number of letters). Specifically, T word length (stem + morpheme) was  $7.98$  (mean)  $\pm 1.08$  (median: 8), PT was  $6.56$  (mean)  $\pm 1.01$  (median: 7), and PS was  $6.25$  (mean)  $\pm 1.08$  (median: 7), respectively. ANOVA revealed a statistically significant difference between the three observations ( $P = 0.001$  corrected; post hoc *t*-tests pointing out the difference between T and PT or PS ( $P < 0.001$  corrected), but not between PT and PS [ $P = 0.43$ ]). Such a mismatch could potentially heavily confound the reported findings, as the latter may be driven by such a mismatch instead of by morphological unification in itself. Hence, oscillatory power at the coordinates and time-frequency of interest (T vs. NT effect reported in Fig. 3B, right panel) were then subjected to a computation of correlation with word length (and frequency) on a trial-by-trial basis. Mean Spearman correlation between power and total word (stem + morpheme) length for the T condition was  $r = 0.01$  ( $P = 0.71$ ), while for the NT condition it was  $r = 0$  ( $P = 0.80$ ). Specifically, in the T condition, power was neither correlated with stem length ( $r = 0$ ,  $P = 0.80$ ) nor was it correlated with morpheme length ( $r = 0.04$ ,  $P = 0.34$ ). The same pattern was also observed in the NT condition for both stem ( $r = -0.03$ ,  $P = 0.20$ ) and morpheme ( $r = 0.03$ ,  $P = 0.26$ ). Additionally, although the conditions did not differ in terms of their lemma frequency ( $P = 0.71$ ), its correlation with power was also tested: Spearman correlation between power and lemma frequency for the T condition was  $r = 0.03$  ( $P = 0.34$ ), while for the NT condition it was  $r = -0.05$  ( $P = 0.12$ ). Thus, the reported effect was probably orthogonal to the above tested word parameters. To recapitulate, induced NGR modulation in the left posterior occipitotemporal cortex (pLOT) at 260–440 ms is most likely to reflect the retrieval of lexical semantic associations during morphological unification.

## DISCUSSION

We found behavioral and neural evidence pointing out that the unification of truly (compared to pseudo) suffixed words occurred more straightforwardly (shorter RT and higher accuracy), and induced enhanced gamma band activity in the left pLOT. These findings provide sound evidence for the role of the pLOT in enabling the access of lexical semantic associations during morphological unification. We now discuss the results in view of theories of morphological processing, and of prior behavioral find-

ings, as well as of previous time-resolving and space-resolving neuroimaging studies.

The current findings should not be taken explicitly as supporting either one of the present theories of morphological decomposition. Although they do promote the role of semantics during morphological processing, the findings do not lean on testing an orthographic control condition (e.g., *brothel*); hence, based on this findings, one should not make inferences on the role of orthography versus semantics during morphological unification. Furthermore, even if such control were included, the novel approach presented here probes morphology through unification, not through decomposition. This findings suggest that morphology can be investigated using the unification approach. Future application of this novel approach should probe further aspects of morphological processing and thereby contribute to understanding the internal organization of words in the mental storage.

Moreover, and from a methodological point of view, we would like to further note the importance of highlighting the chosen task to be used in an experimental design. For instance, when participants are given more time to process the input stimulus (e.g., in unprimed lexical decision), there is a tendency toward effects being larger in the transparent conditions than in the NT conditions [Beyersmann et al., 2012]. This effect is absent when participants are given little time to process the input stimulus (e.g., in primed lexical decision). Similarly, whereas early morphological processing is independent from semantics for proficient readers (during primed lexical decision), nonproficient readers, such as young children, must rely on semantics even at those early stages [Beyersmann et al., 2012]. Thus, according to this view, the ability to fully extract information out of a single word (determined by the experimental paradigm or alternatively by readers' proficiency), would precisely predict the reliance on semantics during morphological processing. Namely, under partial visual word perception morphological processing would rely only on form (orthography), whereas under full visual word perception, morphological processing would additionally rely on meaning (semantics) [see also Levy et al., 2013]. Accordingly, in this study we probed morphological unification, which similarly to unmasked priming is a paradigm triggering and relying on complete (full) resources of word processing (due to explicit/overt visual stimulation), unlike the early and partial resources during masked priming (due to implicit/covert visual stimulation). This explanation accounts for the hurdled cognitive processing during pseudomorphological processing compared to true morphological processing, as observed in this behavioral results (slower RT and lower accuracy) and in those of previous unmasked priming studies.

As for the dynamics of neuronal processing during morphological access, in the past two decades much effort and advance have been put forward for resolving the temporal dynamics of visual word recognition, particularly through

the application of EEG and MEG imaging. For instance, more than a decade ago it has been shown that orthographic (i.e., letters) visual input, as opposed to nonorthographic (i.e., visual symbols) input, can be processed by the LOT as early as at 150–200 ms post stimulus onset [Nobre et al. 1994; Cohen et al., 2000]. MEG studies were further able to allocate this activity to the LOT [Tarkiainen et al., 2002], and some even claimed that ERFs components related to orthographic processing can be distinguished from those related to morphological processing [Lewis et al., 2011; Solomyak and Marantz, 2009, 2010]. Those authors claimed that the recognition of morphological units (i.e., morphological processing) occurs several dozens of milliseconds after that of orthographic units, and is insensitive to the semantic entries which occur later, at approximately 300 ms. Moreover, in a recent visible-prime lexical decision ERP study, the N400 diverged between the NT and the transparent conditions only after 380 ms [Lavric et al., 2012]. Another recent ERP study supports the view that semantically independent morphological decomposition occurs before 250 ms, and that only after that time point, brain activity differs based on semantic information [Lavric et al., 2012]. Altogether, most behavioral-coupled-to-electrophysiological research in recent years, points out that morphological decomposition is based initially on orthographic analysis and is only later constrained by semantic information. Furthermore, one should bear in mind the possibility of a first-stage of whole word recognition or of parallel processing, as a recent MEG study showed simultaneous early activity in the LOT and in frontal language areas which often reflect semantic access [Cornelissen et al., 2009].

In this study, semantic-dependent morphological unification peaked at 260–440 ms, overall corroborating the evoked-component literature aforementioned. Although this finding is not at odds with the form-then-meaning account, we contend that it is certainly not aptly favoring one theory over another regarding the temporal dynamics of morphological processing. Instead, this results show that the unification of morphemic constituents into a single word certainly accesses semantics, and that this occurs not very early in the pLOT, a hub of word processing. Nevertheless, one could speculate that the effect observed here may be driven by automatic lexical processing by the visual perception of the stem at 0 ms, rather than by morphological unification itself. To test for this hypothesis, NT trials were pooled as trials with meaningful (e.g., *pal*) and meaningless (e.g., *kev*) stems. If NGR activity in the pLOT were due to automatic lexical processing, then we would expect to observe enhanced activity for the meaningful stem condition (*pal*, NT) compared to the meaningless stem condition (*kev*, PS); likewise, NT activity would not differ between T and NT. If by contrast, NGR activity were due to a semantic access specific to morphological unification (i.e., T) then we would expect NT and PS to yield a similar level of activation, and an enhanced level of activation for T compared to both NT and PS. The

analysis revealed that NGR activity in the coordinates of interest significantly increased at 260–440 ms during the T condition compared to both NT and PS combined (Fig. 3B) and that there was no difference between the NT and PS conditions. Yet stem presentation could probably trigger earlier cognitive processing such as automatic early word form recognition [related to the so-called “Word Superiority Effect,” see Cattell, 1886], and shown previously [see for instance Cornellison et al., 2009, or Pammer et al., 2004]. Such an effect would most likely be mirrored by contrasting PT versus PS (i.e., real stem versus pseudo-stem); however, our analyses revealed that the observed effect (in the pLOT) was unchanged in the two conditions. Still, because of the relatively late effect in the pLOT, it is not implausible that the latter region is being downstream modulated by earlier differential activity elsewhere in the language system. Hence, other neuronal populations could also play a role in morphological unification, although one should also keep in mind that the heavy cognitive load imposed by this paradigm is suggestive of selective language processing occurring only late in time. Similarly in a previous experiment imposing heavy load due to semantic decision at the threshold of visual recognition, we reported specific effects not earlier than 500 ms post stimulus onset [Levy et al., 2013]. Future studies probing unification may reveal such other putative neuronal dynamics. Nevertheless, these analyses altogether highlight a neural signature in the gamma band in the posterior ventral LOT, signaling semantic access during real morphological unification, as opposed to pseudomorphological unification which does not rely on semantic information. This neural signature cannot be explained by a mere automatic lexical processing (stem perception), although it cannot be ruled out that other earlier processes may be implicated. The specificity to T items suggests that this effect relates to the effective stem-morpheme unification, giving rise to a valid derivative word from a given stem.

Furthermore, there is an ongoing debate around the selectivity of the LOT for word reading [see Dehaene and Cohen, 2011; vs. Price and Devlin, 2011; Price, 2012; Vogel et al., 2012]. Nevertheless, ample body of neuroimaging evidence unequivocally supports the view that this region is largely involved in written word processing, without making claims on its specificity to written words versus other visual categories. In this study, we found that this region had a preferential modulatory effect in the gamma band for true morphological unification, namely, the assembling process of a stem with its associated morpheme (e.g., “rijp” + “ing”). This effect was significantly less robust for the control condition which consisted in unifying stem and morpheme with a pseudomorphological dependence (e.g., “pal” + “ing”). This could be indicative of the successful semantic addition required for true morphological unification, in contrast to a pseudounification in which a morpheme (e.g., *ing*) bears no semantic valence that could complement that of the stem (e.g., *pal*). Previous fMRI/MEG studies have highlighted the role of the LOT in

morphological processing [Bick et al., 2011; Gold and Rastle, 2007; Lewis et al., 2011]. Noteworthy, although the localization of the effect was assigned here to the pLOT, one should consider that the effect may also include the anterior LOT; in that case, the effect may include neuronal populations in the so-called visual word form area [Cohen et al., 2000]. Nevertheless, given the inverse problem of source localization using MEG data, we wish not to be making any strong claims regarding the precision of the effect's localization. Bearing in mind this limitation in precisely localizing cerebral activity, this results are compatible with a posterior-to-anterior functional view of the organization in the LOT, according to which the posterior LOT would rather process word subunits whereas the anterior LOT would process whole words [Binder et al., 2006; Vinckier et al., 2007]. Furthermore, these findings further support role of the pLOT as a mediator of morphemic/sublexical and semantic access [Levy et al., 2009].

Despite highlighting the prominent role of the LOT in visual language processing, including during morphological unification, we would like to note as well the role of the left inferior frontal gyrus (LIFG) for morphological processing: morphological processing was found to prominently recruit the LIFG, as measured by a series of fMRI experiments [Bozic et al., 2010], and by intracranial recordings from epileptic patients during presurgical preparation [Sahin et al., 2009; see also comments by Hagoort and Levelt, 2009]. These different spatial findings can be reconciled by the differences in tasks' modalities and requirements: meta-morphemic lexical-decision task (in this study), compared to silent word utterance [Sahin et al., 2009] and to speech comprehension [Bozic et al., 2010]. Specifically, the meta-morphemic lexical decision task has likely triggered major lexico-semantic processes. Much prior evidence [for a review, see Price and Devlin, 2011] has shown that during reading, the LOT acts as an interface between visual information (processed in the occipital cortex) and higher-level linguistic (phonological and semantic) processing (processed in the frontal cortex). It is, therefore, likely that the high processing load posed on the LOT emanated from the large demand to bridge the visual morphemic entries with lexico-semantic processing. Interestingly, the time frame of the morphological effect as detected here provides a relatively accurate overlap with that reported by Sahin et al., namely peaking at ~320 ms [Sahin et al., 2009]. These lines of research altogether convey the complexity to grasp the full spatiotemporal profile of language processing, and rather converge to point out the necessity to adapt a dynamical systems approach [for a neurobiological model of language comprehension and production, see Hagoort, 2005, 2013]. The brain is dynamic and any specific functional contribution of a given area is dependent on the input it receives from other areas at different time points. Although one can claim the contribution of a specific region (e.g., LOT or LIFG), it is crucial to realize that it is highly dependent on the interactions within the whole network at different time frames and frequency ranges.

On a final note, in addition to outlining the preferential role of NGR in the pLOT for supporting morphological processing, gamma band oscillations in other time-frequency windows were also spotted and were suspected to be attributed to other processes during the task of word reassembling. Namely, early BGR was measured in the bilateral visual cortex, while late NGR was identified in the left premotor cortex. This is consistent with other studies on the gamma frequency band which distinguish genuine gamma oscillations from mere increases of gamma-band power. A proper distinction should, therefore, be made between BGR and NGR as they are likely to reflect different mechanisms [Buzsaki and Wang, 2012] and originate from different biophysical processes [Ray and Maunsell, 2011]. Specifically, BGR could be taken as a reliable electrophysiological index of neuronal firing, whereas NBR would reflect gamma oscillations and could inform us about neuronal population dynamics during various cognitive functions. As BGR provide an excellent indicator of fMRI BOLD response or of neuronal population firing [e.g., Flinker et al., 2011; Hermes et al., 2011; Logothetis et al., 2001; Manning et al., 2009; Miller et al., 2010; Miller, 2010; Parvizi et al., 2012; Ray and Maunsell, 2011], the early BGR activity observed here in the bilateral occipital cortices is most likely a reflection of sensory processing, that is, early visual feature analysis. This is concordant with our previous fMRI study [Levy et al., 2008] which also showed such a response to visual feature analysis in comparison to a pLOT response to orthographic processing. Likewise, late NBR in the motor cortex contralateral to the response press is often observed during tasks implicating motor response [e.g., Donner et al., 2009; Levy et al., 2013], and is, therefore, probably reflecting, in this experiment, the right-hand motor press for the task response. These findings thereby illustrate various neural activities in different time-frequency windows in a broad spectrum of the gamma band, each conveying a different function. Altogether, such perspective is suggestive of the complex and fine-tuned mechanisms across time and frequency sustaining cerebral functioning.

## REFERENCES

- Baayen H, Piepenbrock R, van Rijn H (1993): The CELEX lexical database [CD-ROM]. Philadelphia, PA: University of Pennsylvania, Linguistic Data Consortium.
- Bastiaansen MC, Knösche TR (2000): Tangential derivative mapping of axial MEG applied to event-related desynchronization research. *Clin Neurophysiol* 111:1300–1305.
- Beyersmann E, Coltheart M, Castles A (2012): Parallel processing of whole words and morphemes in visual word recognition. *Q J Exp Psychol (Hove)* 65:1798–1819.
- Bick AS, Goelman G, Frost R (2011): Hebrew brain vs. English brain: Language modulates the way it is processed. *J Cogn Neurosci* 23:2280–2290.
- Binder JR, Medler DA, Westbury CF, Liebenthal E, Buchanan L (2006): Tuning of the human left fusiform gyrus to sublexical orthographic structure. *Neuroimage* 33:739–748.



- Bozic M, Tyler LK, Ives DT, Randall B, Marslen-Wilson WD (2010): Bihemispheric foundations for human speech comprehension. *Proc Natl Acad Sci USA* 107:17439–17444.
- Bresnan JW (2001): *Lexical-Functional Syntax*. Blackwell, Oxford.
- Butterworth B (1983). Lexical representation. In: Butterworth B, editor. *Language Production: Development, Writing, and Other Language Processes*, Vol. 2. London: Academic Press. pp. 257–294.
- Buzsáki G, Draguhn A (2004): Neuronal oscillations in cortical networks. *Science* 304:1926–1929.
- Buzsáki G, Wang XJ (2012): Mechanisms of gamma oscillations. *Annu Rev Neurosci* 35:203–225.
- Cattell JM (1886): The time it takes to see and name objects. *Mind* 11:53–65.
- Chomsky, N (1995): *The Minimalist Program*, MIT Press, Cambridge, Massachusetts/London.
- Cohen L, Dehaene S, Naccache L, Lehericy S, Dehaene-Lambertz G, Henaff MA, Michel F (2000): The visual word form area: Spatial and temporal characterization of an initial stage of reading in normal subjects and posterior split-brain patients. *Brain* 123:291–307.
- Cornelissen PL, Kringelbach ML, Ellis AW, Whitney C, Holliday IE, Hansen PC (2009): Activation of the left inferior frontal gyrus in the first 200 ms of reading: Evidence from magnetoencephalography (MEG). *PLoS One* 4: e5359.
- Crepaldi D, Rastle K, Coltheart M, Nickels L (2010): “Fell” primes “fall”, but does “bell” prime “ball”? Masked priming with irregularly-inflected primes. *J Mem Lang* 63:83–99.
- Crone NE, Miglioretti DL, Gordon B, Lesser RP (1998): Functional mapping of human sensorimotor cortex with electrocorticographic spectral analysis: II. Event-related synchronization in the gamma band. *Brain* 121:2301–2315.
- Dehaene S, Cohen L (2011): The unique role of the visual word form area in reading. *Trends Cogn Sci* 15:254–262.
- Diependaele K, Sandra D, Grainger J (2009): Semantic transparency and masked morphological priming: The case of prefixed words. *Mem Cogn* 37:895–908.
- Donner TH, Siegel M (2011): A framework for local cortical oscillation patterns. *Trends Cogn Sci* 15:191–199.
- Donner TH, Siegel M, Fries P, Engel AK (2009): Buildup of choice-predictive activity in human motor cortex during perceptual decision making. *Curr Biol* 19:1581–1585.
- Engel AK, Singer W (2001): Temporal binding and the neural correlates of sensory awareness. *Trends Cogn Sci* 5:16–25.
- Feldman LB, O'Connor PA, Moscoso del Prado Martin F (2009): Early morphological processing is morpho-semantic and not simply morpho-orthographic: Evidence from the masked priming paradigm. *Psychon Bull Rev* 16:684–691.
- Flinker A, Chang EF, Barbaro NM, Berger MS, Knight RT (2011): Subcentimeter language organization in the human temporal lobe. *Brain Lang* 117:103–109.
- Foster BL, Parvizi J (2012): Resting oscillations and cross-frequency coupling in the human posteromedial cortex. *Neuroimage* 60:384–391.
- Gaillard R, Dehaene S, Adam C, Clémenceau S, Hasboun D, Baulac M, Cohen L, Naccache L (2009): Converging intracranial markers of conscious access. *PLoS Biol* 7:e61.
- Giraudo H, Grainger J (2001): Priming complex words: Evidence for supralexical representation of morphology. *Psychon Bull Rev* 8:127–131.
- Gold B, Rastle K (2007): Neural correlates of morphological decomposition during visual word recognition. *J Cogn Neurosci* 19:1983–1993.
- Gross J, Kujala J, Hämäläinen M, Timmermann L, Schnitzler A, Salmelin R (2001): Dynamic imaging of coherent sources: Studying neural interactions in the human brain. *Proc Natl Acad Sci USA* 98:694–699.
- Hagoort P (2005): On Broca, brain, and binding: A new framework. *Trends Cogn Sci* 9:416–423.
- Hagoort P (2013): MUC (Memory, Unification, Control) and beyond. *Front Psychol* 4:416.
- Hagoort P, Levelt WJM (2009): The speaking brain. *Science* 326:372–373.
- Hämäläinen M, Hari R, Ilmoniemi RJ, Knuutila J, Lounasmaa OV (1993): Magnetoencephalography—Theory, instrumentation, and applications to noninvasive studies of the working human brain. *Rev Mod Phys* 65:413–497.
- Hermes D, Miller KJ, Vansteensel MJ, Aarnoutse EJ, Leijten FS, Ramsey NF (2011): Neurophysiologic correlates of fMRI in human motor cortex. *Hum Brain Mapp* 33:1689–1699.
- Jackendoff, R. (2002) *Foundations of Language: Brain, Meaning, Grammar, Evolution*. Oxford: Oxford University Press.
- Joshi AK, Schabes Y (1997): Treeadjoining grammars. In: Salomaa A, Rosenberg G, editors. *Handbook of Formal Languages and Automata*, Vol. 3. Springer, Berlin. pp. 69–124.
- Lachaux JP, Axmacher N, Mormann F, Halgren E, Crone NE (2012): High-frequency neural activity and human cognition: Past, present and possible future of intracranial EEG research. *Prog Neurobiol* 98:279–301.
- Lavric A, Clapp A, Rastle K (2007): ERP evidence for morphological analysis from orthography: A masked priming study. *J Cogn Neurosci* 19:866–877.
- Lavric A, Elchlepp H, Rastle K (2012): Tracking hierarchical processing in morphological decomposition with brain potentials. *J Exp Psychol Hum Percept Perform* 38:811–816.
- Lehtonen M, Monahan PJ, Poeppel D (2011): Evidence for early morphological decomposition: Combining masked priming with magnetoencephalography. *J Cogn Neurosci* 23:3366–3379.
- Levy J, Pernet C, Treserras S, Boulanouar K, Berry I, Aubry F, Demonet JF, Celsis P (2008): Piecemeal recruitment of left-lateralized brain areas during reading: A spatio-functional account. *Neuroimage* 43:581–591.
- Levy J, Pernet C, Treserras S, Boulanouar K, Aubry F, Demonet JF, Celsis P (2009): Testing for the dual-route cascade reading model in the Brain: An fMRI effective connectivity account of an efficient reading style. *PLoS ONE* 4:e6675.
- Levy J, Vidal JR, Oostenveld R, Fitzpatrick I, Démonet JF, Fries P (2013): Alpha-band suppression in the visual word form area as a functional bottleneck to consciousness. *Neuroimage* 78:33–45.
- Lewis G, Solomyak O, Marantz A (2011) The neural basis of obligatory decomposition of suffixed words. *Brain Lang* 118(3):118–127. doi: 10.1016/j.bandl.2011.04.004.
- Logothetis NK, Pauls J, Augath M, Trinath T, Oeltermann A (2001): Neurophysiological investigation of the basis of the fMRI signal. *Nature* 412:150–157.
- MacDonald MC Pearlmuter NJ, Seidenberg MS (1994): Lexical nature of syntactic ambiguity resolution. *Psychol Rev* 101:676–703.
- Mainy N, Jung J, Baciú M, Kahane P, Schoendorff B, Minotti L, Hoffmann D, Bertrand O, Lachaux JP (2008): Cortical dynamics of word recognition. *Hum Brain Mapp* 29:1215–1230.

- Manning JR, Jacobs J, Fried I, Kahana MJ (2009): Broadband shifts in local field potential power spectra are correlated with single-neuron spiking in humans. *J Neurosci* 29:13613–13620.
- Maris E, Oostenveld R (2007): Nonparametric statistical testing of EEG- and MEG-data. *J Neurosci Meth* 164:177–190.
- Martin CD, Thierry G (2008): Interplay of orthography and semantics in reading: An event-related potential study. *Neuroreport* 19:1501–1505.
- Martin CD, Thierry G, Démonet JF (2010): ERP characterization of sustained attention effects in visual lexical categorization. *PLoS One* 5:e9892.
- Miller KJ (2010): Broadband spectral change: Evidence for a macroscale correlate of population firing rate? *J Neurosci* 30:6477–6479.
- Miller KJ, Hermes D, Honey CJ, Sharma M, Rao RP, den Nijs M, Fetz EE, Sejnowski TJ, Hebb AO, Ojemann JG, Makeig S, Leuthardt EC (2010): Dynamic modulation of local population activity by rhythm phase in human occipital cortex during a visual search task. *Front Hum Neurosci* 4:197.
- Morris J, Frank T, Grainger J, Holcomb PJ (2007): Semantic transparency and masked morphological priming: An ERP investigation. *Psychophysiology* 44:506–521.
- Morris J, Grainger J, Holcomb PJ (2008): An electrophysiological investigation of early effects of masked morphological priming. *Lang Cogn Processes* 23:1021–1056.
- Nichols TE, Holmes AP (2002): Nonparametric permutation tests for functional neuroimaging: A primer with examples. *Hum Brain Mapp* 15:1–25.
- Nobre AC, Allison T, McCarthy G (1994): Word recognition in the human inferior temporal lobe. *Nature* 372:260–263.
- Nolte G (2003): The magnetic lead field theorem in the quasi-static approximation and its use for magnetoencephalography forward calculation in realistic volume conductors. *Phys Med Biol* 48:3637–3652.
- Oostenveld R, Fries P, Maris E, Schoffelen JM (2011): FieldTrip: Open source software for advanced analysis of MEG, EEG, and invasive electrophysiological data. *Comput Intell Neurosci* 156869. doi: 10.1155/2011/156869.
- Pammer K, Hansen PC, Kringelbach ML, Holliday I, Barnes G, Hillebrand A, Singh KD, Cornelissen PL (2004): Visual word recognition: The first half second. *Neuroimage* 22:1819–1825.
- Parvizi J, Jacques C, Foster BL, Withoft N, Rangarajan V, Weiner KS, Grill-Spector K (2012): Electrical stimulation of human fusiform face-selective regions distorts face perception. *J Neurosci* 32:14915–14920.
- Percival DB, Walden AT (1993): *Spectral Analysis for Physical Applications: Multitaper and Conventional Univariate Techniques*. Cambridge, UK: Cambridge University Press.
- Price CJ (2012): A review and synthesis of the first 20 years of PET and fMRI studies of heard speech, spoken language and reading. *Neuroimage* 62:816–847.
- Price C, Devlin JT (2011): The interactive account of ventral occipitotemporal contributions to reading. *Trends Cogn Sci* 15:246–253.
- Pylkkänen L, Marantz A (2003): Tracking the time course of word recognition with MEG. *Trends Cogn Sci* 7:187–189.
- Rastle K, Davis MH, Marslen-Wilson WD, Tyler LK (2000): Morphological and semantic effects in visual word recognition: A time course study. *Lang Cogn Processes* 15:507–537.
- Rastle K, Davis MH, New B (2004): The broth in my brother's brothel: Morpho-orthographic segmentation in visual word recognition. *Psychon Bull Rev* 11:1090–1098.
- Ray S, Maunsell JH (2011): Different origins of gamma rhythm and high-gamma activity in macaque visual cortex. *PLoS Biol* 9:e1000610.
- Roelfsema PR, Lamme VA, Spekreijse H (1998): Object-based attention in the primary visual cortex of the macaque monkey. *Nature* 395:376–381.
- Sahin NT, Pinker S, Cash SS, Schomer D, Halgren E (2009): Sequential processing of lexical, grammatical and phonological information within broca's area. *Science* 326:445–449.
- Solomyak O, Marantz A (2009): Lexical access in early stages of visual word processing: A single-trial correlational MEG study of heteronym recognition. *Brain Lang* 108:191–196.
- Solomyak O, Marantz A (2010): Evidence for early morphological decomposition in visual word recognition. *J Cogn Neurosci* 22:2042–2057.
- Taft M (2003): Morphological representation as a correlation between form and meaning. In: Assink E, Sandra D, editors. *Reading Complex Words*. Amsterdam, The Netherlands: Kluwer. pp. 113–137.
- Taft M, Forster KI (1975): Lexical storage and retrieval of prefixed words. *J Verbal Learning Verbal Behav* 14:638–647.
- Tallon-Baudry C, Bertrand O (1999): Oscillatory gamma activity in humans and its role in object representation. *Trends Cogn Sci* 3:151–162.
- Tarkiainen A, Cornelissen PL, Salmelin R (2002): Dynamics of visual feature analysis and object-level processing in face versus letter-string perception. *Brain* 125:1125–1136.
- Thierry G, Doyon B, Démonet JF (1998): ERP mapping in phonological and lexical semantic monitoring tasks: A study complementing previous PET results. *Neuroimage* 8:391–408.
- Thierry G, Cardebat D, Démonet JF (2003a): Electrophysiological comparison of grammatical processing and semantic processing of single spoken nouns. *Brain Res Cogn Brain Res* 17:535–547.
- Thierry G, Ibarrola D, Démonet JF, Cardebat D (2003b): Demand on verbal working memory delays haemodynamic response in the inferior prefrontal cortex. *Hum Brain Mapp* 19:37–46.
- Vidal JR, Freyermuth S, Jerbi K, Hamamé CM, Ossandon T, Bertrand O, Minotti L, Kahane P, Berthoz A, Lachaux JP (2012): Long-distance amplitude correlations in the high gamma band reveal segregation and integration within the reading network. *J Neurosci* 32:6421–6434.
- Vidal JR, Perrone-Bertolotti M, Levy J, De Palma L, Minotti L, Kahane P, Bertrand O, Lutz A, Jerbi K, Lachaux JP (2014): Neural repetition suppression in ventral occipito-temporal cortex occurs during conscious and unconscious processing of frequent stimuli. *Neuroimage* 95:129–135.
- Vinckier F, Dehaene S, Jobert A, Dubus JP, Sigman M, Cohen L (2007): Hierarchical coding of letter strings in the ventral stream: dissecting the inner organization of the visual word-form system. *Neuron* 55:143–156.
- Vogel AC, Petersen SE, Schlaggar BL (2012): The left occipitotemporal cortex does not show preferential activity for words. *Cereb Cortex* 22:2715–2732.
- Vosse T, Kempen GAM (2000): Syntactic structure assembly in human parsing: A computational model based on competitive inhibition and lexicalist grammar. *Cognition* 75:105–143.
- Voytek B, Canolty RT, Shestyuk A, Crone NE, Parvizi J, Knight RT (2010): Shifts in gamma phase-amplitude coupling frequency from delta to alpha over posterior cortex during visual tasks. *Front Hum Neurosci* 4:191.